Combined Delivery of Temozolomide and Anti-miR221 PNA Using Mesoporous Silica Nanoparticles Induces Apoptosis in Resistant Glioma Cells

DOI: 10.1002/ ((please add manuscript number))
Full paper

Combined delivery of temozolomide and anti-miR221 PNA using mesoporous silica nanoparticles induces apoptosis in resistant glioma cells

Alessandro Bertucci, Eko Adi Prasetyanto, Dedy Septiadi, Alex Manicardi, Eleonora Brognara, Roberto Gambari, Roberto Corradini*, Luisa De Cola**

A. Bertucci, Dr. E.A. Prasetyanto, D. Septiadi, Prof. L. De Cola
Institut de science et d'ingénierie supramoléculaire (ISIS)
Université de Strasbourg,
8 Alléè Gaspard Monge, Strasbourg, 67000, France
decola@unistra.fr

A. Bertucci, Dr. A. Manicardi, Prof. R. Corradini
Dipartimento di Chimica
Università di Parma
Parco Area delle Scienze 17/A, Parma, 43124, Italy
roberto.corradini@unipr.it

Dr. E. Brognara, Prof. R. Gambari
Dipartimento di Scienze della Vita e Biotecnologie
Università di Ferrara
Via Luigi Borsari 46, Ferrara, 44121, Italy
roberto.gambari@unife.it

Keywords: nanomaterials, nanomedicine, microRNA, drug resistance, PNA

Abstract

Mesoporous silica nanoparticles (MSNPs), 100 nm in size, incorporating a Cy5 fluorophore within the silica framework, were synthesized and loaded with the anti-cancer drug temozolomide (TMZ), used in the treatment of gliomas. The surface of the particles was then decorated, using electrostatic interactions, with a polyarginine-peptide nucleic acid (R8-PNA) conjugate targeting the miR221 microRNA. The multi-functional nanosystem thus obtained was rapidly internalized into glioma C6 or T98G cells. The anti-miR activity of the PNA was retained, as measured by RT-PCR measurements. Induction of apoptosis was observed in

temozolomide-resistant cell lines. TMZ-loaded MSNP showed an enhanced pro-apoptotic effect, and the combined effect of TMZ and R8-PNA in MSNP showed the most effective induction of apoptosis (70.9% of apoptotic cells) in the temozolomide-resistant T98G cell line.

1. Introduction

The administration of an efficient cancer therapy still remains a substantial goal, since the traditional use of a single therapeutic strategy in many cases might not represent the optimal way to provide a complete and effective cure. The combination of chemotherapeutic agents has also been used to prevent drug resistance, but the ability of cancer cells to adapt and develop new resistance pathways eventually leads to feeble results.[1,2] On the other hand, a very interesting and promising strategy for an efficient cancer treatment relies on the combination of two or more therapeutic approaches with diverse mechanisms, which can synergistically cooperate to give an enhanced final therapeutic effect.[3-7] For this reason, considerable efforts have been devoted to the development of strategies based on the combination of traditional drug-based chemotherapy with the emergent RNA-interference-based therapy (RNAi) and miRNA therapeutics, which allows for selectively targeting and downstream regulating RNA targets involved in the tumor proliferation and in its drug resistance. The advent of nanotechnology has indeed played a key role towards this aim, leading to the design and fabrication of multi-structured nanomaterials tailored in such a way to carry and to deliver the therapeutic components in a sustainable manner directly to the cells.[8-13] The use of nano-carriers has been described for the simultaneous delivery of siRNA or miRNA and anti-cancer drugs[13] greatly enhancing the possibility to reduce drug resistance in tumors.[14] Among others, mesoporous silica nanoparticles (MSNPs) have been considered as one of the most promising platforms for the realization of multifunctional delivery systems, thanks to their large surface area with well-defined chemical properties, their controllable and tunable porous structure for hosting guest molecules, and their excellent biocompatibility.[15-

[19] The behavior of MSNPs *in vivo* has been also thoroughly investigated, and it has been pointed out how the intrinsic properties of the particles and the subsequent chemical modifications deeply influence biodistribution, biodegradation, and definitive clearance. Although few adverse reports, it is a common view that MSNPs are suitable platforms for being used *in vivo,* and numerous studies have been carried out with this strategy.[20] Multivalent MSNPs has been shown to be suitable for the combination of drug and RNAi[14,21,22] treatments; for example the double release of doxorubicin and specific siRNA by MSNPs to overcome drug resistance in breast cancer or HeLa cells has been demonstrated.[23,24] Recently, also microRNAs (miRNAs or miRs) have emerged as potentially powerful targets for gene modulation. MiRNAs are short non-coding RNA molecules that regulate gene expression by repressing translation or by inducing the cleavage of target RNA transcripts.[25,26] Emerging evidences suggest that the abnormal expression profile of miRNAs can be correlated to the pathogenesis of cancer,[27,28] to tumor progression, and to drug resistance. The anti-miR strategy (miRNA targeting therapy) can be very useful in the treatment of tumors overexpressing a specific type of miR; however, due to the presence of multiple targets, the effect of a single anti-miR molecule in most cases might have a limited effect. Combined therapies can thus be used, especially in cases where the target miR is correlated with chemo-resistance. One of the possible miRNA targets, miR-221, has been found to be upregulated in several tumor forms,[29-31] and especially in gliomas.[32-34] It was shown to regulate several key target genes, among which $p27^{Kip1}$ mRNA appears to be one of the most interesting, since this protein is a strong regulatory element able to modulate cyclin-CDK complex activity and hence cell cycle progression;[35] miR-221 knock-down can potentially trigger $p27^{Kip1}$ upregulation.[36-38] Interestingly, the dowregulation of miR-221 has been shown to sensitize glioma cells to temozolomide, which is one of the most common antineoplastic agents for malignant glial tumors.[39-41]

In this work we report, for the first time, the use of multifunctional MSNPs for the concomitant delivery of anti-miR-221 PNA-octaarginine conjugate (R8-PNA221) and temozolomide to drug resistant glioma cells, demonstrating increased biological effects of the two agents when administered in combination. The role played by the R8-PNA221 and temozolomide separately, and the comparison with the nanomaterial containing both the active components help to clarify the effect of miR221 inhibition on temozolomide resistance and clearly demonstrate the efficacy of the system on inducing apoptosis in cancer cells.

2. Results and discussion

2.1. Material design, multi-functionalization, and characterization

MiR221 is one of the most studied molecular targets in oncology research, being overexpressed in a large variety of tumors, and is associated to poor prognosis[42] due to its effect on several important targets, such as p27Kip1, TIMP3, TRAIL and PTEN. In gliomas, miR 221 has been associated to invasiveness[43] and resistance to temozolomide.[39] Furthermore, miR 221 is elevated in radioresistant tumor cell lines.[44]

Among the possible available tools for anti-miR targeting, peptide nucleic acids (PNAs)[45-47] represent an excellent choice. PNAs, due to their high affinity for the nucleic acid, their sequence selectivity, and their high stability towards both chemical and biological degradation, have been used as antisense agents and have been shown to be able to efficiently target miRNAs.[48-52] We thus chose PNA as anti-miR component to be used in combination with mesoporous silica nanoparticles. Furthermore, the overall charge of PNAs can easily be tuned either by conjugation with suitable peptides (directly introduced during PNA solid-phase synthesis), or by a modification of the backbone with charged substituents;[53] thus, unlike other oligonucleotide analogs, PNAs allow to finely tune the overall charge of the nanosystem to positive or mildly negative values, and thus suitable for cellular uptake. A suitable

fluorophore (Cyanine-5, Cy5) was embedded in the mesoporous silica matrix allowing for the localization of the nanoparticles inside the cells.

The schematic view of the whole fabrication of multi-functionalized mesoporous silica nanoparticles is reported in Figure 1.

MSNPs of 100 nm in diameter were synthesized following a typical sol-gel micelle-templated process[53] described in the experimental section. The size range of the particles represents a good regime for efficient cellular uptake as previously reported.[55-57] The red cyanine 5 dye was directly grafted into the silica network; a one-pot synthesis was carried out using a Cy5-NHS-ester and a small fraction of (3-aminopropyl)triethoxysilane (APTES), which made it possible to covalently embed the dye into the silica structure. This dye was selected since its emission does not overlap with all the other signals involved in the cellular uptake experiments and the biological tests (e.g. Alexa Fluor® 568 Phalloidin used for staining f-actin filaments).

Due to the template synthesis the presence of the surfactant in the pores plays a crucial role for the external surface functionalization, preventing the silane derivative to react also with the –OH groups of the internal surface of the pores, which may lead to an obstruction of the empty channels. Functionalization of the nanoparticles is achieved using (3-aminopropyl)-dimethyl-ethoxysilane (APDMS) to provide amine-functionalization of the particle surface by simple silane chemistry. At this point, templating cetyl trimethylammonium bromide (CTAB) is totally removed by an overnight treatment with acidic ethanol (see Figure 1). The final zeta potential value of +7.96 mV, obtained at this step, clearly indicate the presence of the amine functional groups on the outer surface of the particles, due to protonated amino groups. The coverage of the surface with amino groups was also corroborated by the positive ninhydrin test. Subsequently, the amino groups were converted into carboxylic acids by reaction with succinic anhydride, which was again confirmed by a zeta potential shift to -36.42 mV. The presence of a total negative charge on the particle surface is indeed crucial for the final step,

involving electrostatic binding of the cationic anti-miR221 PNA. Temozolomide was then loaded into the particle pores. Due to the low molecular weight of the drug, which can be uptaken and released from the pores, an impregnation strategy involving evaporation of the working solution and washing with solvents showing different solubility for TMZ was performed as described in the experimental section, which allowed us to achieve a final loading value of 17% (*wt/wt*). This value was calculated by means of UV-Vis spectroscopy,[58] following residual temozolomide absorption in the UV region after the loading procedure (see supporting information for details). A batch of these TMZ-particles was used as such during the cell experiments, while a further functionalization step was carried out on few mg to achieve the final PNA decoration. Thus, once MSNPs were filled up with the drug, R8-PNA221 could finally be bound to the nanocarriers. Due to the cationic nature of the arginine-modified PNA probes, they were electrostatically adsorbed on the negatively charged surface of carboxylated-functionalized MSNPs, by dispersing the particles in the aqueous PNA solution. From a targeting point of view, the adoption of cationic PNAs helps to enhance the hybridization properties of the probes by additionally exploiting electrostatic interaction.[46,59] Moreover, the presence of cationic species on the particle surface directly improves the cellular uptake of the nanosystem, without further need of cationic polymer coatings.[60] Furthermore, the use of cationic PNAs leads to a reduction in the number of steps otherwise required for a covalent binding of the probes to the particle surface. In addition, the PNA coating can mimic the pore blocking effect achieved when using DNA oligos,[61,62] and serves to inhibit a progressive unwanted release of the drug and to help control the release of temozolomide. After R8-PNA221 adsorption, the zeta potential of the particles was considerably shifted reaching a value of +0.34 mV, which indeed proved the successful binding of the PNAs to MSNPs. PNA loading was evaluated by UV-Vis spectroscopy monitoring the absorption peak at 260 nm before and after incubation with the

negatively charged particles, and was found to be 3.6 nanomoles per mg of material (corresponding to 15 μg PNA/mg MSNP).

For comparison, and to evaluate the gaining of the full system containing both TMZ and PNA, the MSNPs loaded only with temozolomide, TMZ-MSNPs and nanomaterials decorated only with R8-PNA221, PNA-MSNPs, have also been used. The TMZ-MSNPs were prepared as mentioned above. The zeta potential of the material was -35.26 mV, indicating no residual drug adsorbed on the surface. The PNA-MSNPs were synthesized following the same procedure, but skipping the TMZ-loading step. A zeta potential value of +0.11 mV showed the success of the surface coating. The particles have been extensively characterized with SEM, TEM, SAXS, zeta potential, fluorescence spectroscopy, dynamic light scattering (DLS), and confocal microscopy (see Figure 1 and S1-5). The SAXS pattern of the mesoporous material without surfactants is shown in Figure S2. The sample shows three clear diffraction peaks, which can be indexed to a 2D-hexagonal lattice. SEM and TEM measurements (Figure 1) clearly show the homogeneity and porosity of the materials.

2.2. Cellular uptake and cytotoxic effect in glioma C6 cells

In order to address the interaction between the nanosystem, containing both temozolomide and PNA, PNA-TMZ-MSNPs, and live cells, a C6 glioma cell line was used. Cell experiments were carried out incubating C6 glioma cells (approximately 50,000 cells/plate) for 1, 4, and 24 hours, using a particle concentration of 0.05 mg/mL. After incubation, the cells were washed, fixed, and analyzed by confocal microscopy (Figure 2). Visualization and tracking of the nanoparticles inside the cells was possible by monitoring, with confocal microscopy, the red fluorescence of the cyanine 5 dye inserted in the silica scaffold during the synthesis. Additionally, for a better view of the cell shape, we also stained the actin filaments with Alexa Fluor® 568 Phalloidin, after cell fixation, whose emission does not overlap with that of Cy5. The results, summarized in Figure 2, show that already after 1 hour a significant

number of nanoparticles can be visualized inside the cells, proving that the system is properly tailored for an efficient (i.e. fast) cellular uptake.

A prolongation in incubation time led to an increase in particle concentration in the cell cytoplasm. Particle uptake was confirmed by recording Z-stack images (Fig. 2D). It is worth to note that unmodified PNAs generally show poor cell membrane permeability,[63] and uptake of silica nanoparticles is strongly affected by their size, shape, and surface properties[64,65]. It is generally accepted that the induction of a net positive charge on the surface of the nanoparticles tends to facilitate the internalization process;[60,64] on this account, positively charged polymer has been frequently used as coating layers to improve cellular uptake.[23,58,66] In our case, the use of a cationic PNA on silica nanoparticles is intended to provide a similar outcome, promoting cell uptake of the functional nanocarrier without the need for an-extra polymer coating.

As a first tests for studying the biological and possible cytotoxic effect of our multimodal system, cell viability experiments were carried out on C6 glioma cells incubated with different combinations of Cy5-labelled PNA-TMZ-MSNPs. It has been recently found that this glioma cell line tends to overexpress the onco-miR221, which is involved in the tumor proliferation.[32,66,68] C6 glioma cell line is also resistant to temozolomide treatment, which makes it a suitable candidate to investigate the therapeutic potentialities of our PNA-TMZ-MSNP system.[69-71] For a better comprehension of the efficacy of this approach and to prove the synergistic effect of the therapeutic molecules a complete set of experiments was designed, incubating the cell for 24 and 48 hours with, respectively, MSNPs filled with temozolomide only (TMZ-MSNPs), MSNPs modified with R8-PNA221 only (PNA-MSNPs), and MSNPs loaded with temozolomide and coated with the R8-PNA221 (PNA-TMZ-MSNPs). At the end of each of incubations, cells were trypsinized and cell pellets were harvested. The total cell viability was measured as a direct indication of the cytotoxic effect of the material. After 24 hours, TMZ-MSNPs and PNA-MSNPs provided a modest effect while, very interestingly, the

combined delivery of the drug and the anti-miR PNA (PNA-TMZ-MSNPs) determined a drastic reduction in the cell viability, up to a 30% value (see Fig. S7). After 48 hours, a visible reduction of cell viability was also observed for TMZ-MSNPs and PNA-MSNPs, but still a much greater reduction was obtained for PNA-TMZ-MSNPs, which further decreased cell viability to 20% (see Fig. S8). This set of data clearly suggests that the combined delivery of temozolomide and antimiR-221 PNAs provides a synergistic cytotoxic effect to the C6 glioma cells. The efficacy of the presence of both molecules is always higher than the mere sum of the contributions of the two mono-functionalized particles (TMZ-MSNPs and PNA-MSNPs). Hence, due to the very promising results by far obtained, the system was tested also on a TMZ-resistant T98G human glioma cell line.[72]

2.3. Uptake and anti miR-221 activity of PNA-MSNPs in T98G cell line.

The TMZ-resistant T98G cell line was used and exposed to 0.1 and 0.5 mg/ml MSNPs either empty, or carrying TMZ, R8-PNA221 (PNA-MSNPs) and both TMZ and R8-PNA221 (PNA-TMZ-MSNPs). We have previously reported that a mutated R8-PNA221 does not hybridize to miR221 target sequences and has only minor effects on apoptosis, when compared with the full complementary R8-PNA221).[33] All the experiments are depicted in Figure 3 (performed in triplicate). The FACS analysis, shown in Figure 3 A and B, suggests that concentration-dependent uptake is obtained when T98G cells are treated for 24 hours with MSNPs, TMZ-MSNPs, PNA-MSNPs and TMZ-PNA-MSNPs. The data clearly indicate that the cells can uptake almost all of the different MSNP-based formulations.

The anti-miR activity of PNA-MSNPs was tested, in order to establish if the adsorption of the PNA strands on the silica could interfere with the interaction with the target. When the glioma cell line T98G was cultured in the presence of PNA-MSNPs a very reproducible effect was obtained, as shown in Figure 3. The results demonstrate that the miR-221 specific hybridization signal was reduced when RNA was isolated from T98G glioma cell lines cultured for 48 h in the presence of 0.25 mg/ml of PNA-MSNPs. As published elsewhere,[32]

no major effects have been obtained in these experiments using PNA221 or a mutated R8-PNA221; the same is true for the bare MSPN nanoparticles, whereas PNA-MSNPs (0.25 mg/ml, corresponding to 0.9 μM concentration of R8-PNA) induced a significant reduction in the miR221 bioavailability. The lower signal obtained by qRT-PCR for the cationic R8-PNA221, at a comparable concentration as the PNA-MSNPs (1 μM), suggests that the free PNA inhibited miR221 slightly more efficiently than the same PNA bound to the MSNPs (Figure 3, C). Since it was shown that high-affinity anti-miRs, such as PNA, can sequester miRs without causing miRNA degradation,[73] this test measures the competition of PNA and RT-PCR machinery for the target miR, this difference is probably due to delayed release of the PNA from the nanoparticles. Downstream biological effects were thus further evaluated in order to assess the efficiency of the anti-miR R8-PNA in combination with temozolomide treatment.

2.4. Effect of PNA-TMZ-MSNPs on apoptosis of glioma T98G cells

The glioma cell line T98G was cultured in the presence of TMZ. These cells are temozolomide resistant as clearly shown by the dramatic difference observed by comparing the TMZ effects on T98G with the TMZ-sensitive cell lines (such as glioma U251 cells). [33] The representative results shown in Figure 4 and the summary data shown in the insert of Figure 5A confirm, as expected, that TMZ was unable to induce high levels of apoptosis (in particular compare panel C with A and B of Figure 4). On the contrary, as elsewhere reported by some of us, the use of a longer PNA[33] , still R8-PNA221, induced a significant increase of late apoptotic cells (a total of 24.6% in the representative experiment shown in Figure 4D). It should be underlined that exposure to this cell line to unloaded MSNPs causes only a slight increase of apoptosis when 0.5 mg/ml concentrations were used (Figure 4, panel F), being the effects not relevant when lower concentrations (0.1 and 0.25 mg/ml) were employed (Figure 4, panel E and Figure 5A). These results are in line with earlier studies,[74] and were attributed to the induction of oxidative response when high MSNP concentrations were used. In any

case, the data of the treatments depicted in Figures 4 and 5 were reported as % of increase of apoptotic cells in respect to the effects found with unloaded MNSPs. When the data are comparatively analyzed, strong apoptotic effects were clearly evident in T98G cells cultured in the presence of TMZ-MSNPs, PNA-MSNPs and PNA-TMZ-MSNPs (see representative data shown in Figure 4, Figure 5B and the summary analysis shown in panels C and D of Figure 5). In the case of PNA-MSNPs, the comparison of data conclusively show that adsorption on MSNPs does not alter significantly the ability of R8-PNA221 to induce apoptosis in intact cells. Since the PNA-MSNP system showed anti-miR-221 activity, and anti-miR-221 PNA were shown to induce apoptosis, the effect of PNA-MSNP and TMZ-PNA-MSNP reported in figures 4-5 cannot be due solely to the presence of the octaarginine chain. In the case of TMZ delivery, we observed the conversion of T98G cells from TMZ-resistant to TMZ-sensitive when TMZ-MSNPs are used. In fact it is remarkable to have obtained significant increases of the of proportion of apoptotic cells in TMZ-MSNPs treated T98G cells, a value significantly higher that the combined background levels of apoptosis observed in untreated and free-MSNPs treated cells (compare in Figure 4 panels G and H with panels A and F). The enhancement of the effect when the porous materials are used as drug delivery system can be attributed to the sustained release of TMZ, which is protected from clearance by the MSNP and slowly liberated within cells.[75] Interestingly a much larger T98G apoptosis is achieved in the case of 0.5 mg/ml PNA-TMZ-MSNPs, which induced 70.9% total apoptotic cells, with an increase of 50.4% with respect to unloaded MSNPs. The summary of the MSNPs mediated effects are reported in Figure 5, panels B-E; we underline that the 0.5 mg/ml MSNP concentration approaches the reference concentrations of TMZ (400 µM, panel C of Figure 4) and R8-PNA221 (2 µM, panel D of Figure 4).

The effect of PNA-TMZ-MSNPs is already evident at much lower concentration, 0.1 mg/ml, since even in such a condition the PNA-TMZ-MSNPs induced a total of 26.9% apoptotic cells, with an increase of 15.6% with respect to unloaded MSNPs. The values of % of increase of

apoptotic cells in PNA-TMZ-MSNPs treated T98G cells were always foud higher than the sum of the values found in cells treated with PNA-MSNPs and TMZ-MSNPs.

Our data eventually show that PNA-TMZ-MSNPs have the highest impact in inducing the apoptosis of T98G cells, and that the sustained release of temozolomide is not contrasted by the combination with anti-miR221 PNA, but rather that an additional effect can be obtained. Our system thus appears able to provide drug delivery and miRNA-induced downstream regulation of important cell-cycle regulatory proteins. The combined delivery of these two effects has a massive impact on the final apoptosis outcome.

3. Conclusion

Although TMZ offers some hope to glioma patients, presently only a low 5-year survival rate is achieved.[76,77] The anti-miR approach represents a powerful alternative as it is now a major focus in translational research: clinical trials are being carried out for several anti-miR drugs, and, most notably, one clinical trial on humans is currently underway.[78] Although nanocarriers such as MSNPs have been extensively used to enhance the efficiency of drugs through delayed release and protection from clearance (sustained drug release), and artificial DNA analogues such as PNA have been proposed as anti-miR drug candidates, the combination of these two agents has not been explored so far.

The porous nanomaterial synthesized in the present work can protect and slowly deliver the TMZ into the cytoplasm preventing a rapid clearance of the drug; at the same time, it enables the intracellular delivery of the anti-mR221 PNA. The achieved combined delivery leads to a strong induced apoptosis of cancer cells. Therefore the use of TMZ-PNA-MSNPs can be proposed as a novel approach to tackle drug-resistance in gliomas. This is a key issue, since after surgery and radiotherapy, the chemotherapy protocol commonly suffers from the development of drug-resistant glioma cells, as in the case of the usage of TMZ. Since strategies for the delivery of inorganic nanoparticle through the blood-brain-barrier (BBB) have been described (including for instance the use of BBB-penetrating peptides)[79-82] and

MSNP have been reported to accumulate into tumor tissues, the present strategy can be further extended to a multiple-target treatment of gliomas, which are kinds of highly recurrent, frequently drug resistant, and life-threatening tumors.

4. Experimental section

Synthesis of cationic anti-miR-221 PNA (R8-PNA221): The cationic anti-miR-221 PNA H-RRRRRRRR-GCAGACAATGTAGCT-Gly-NH_2 (where R is an arginine residue) was synthesized with standard manual Boc-based chemistry using commercially available monomers, with HBTU/DIPEA coupling as described elsewhere.[83] Details and characterization are reported in the Supporting Information.

Synthesis of MSNPs (Cy5-MSNPs) and loading with PNA and TMZ: **Cy5**-MSNPs were synthesized with a modification of a literature procedure,[84]. Briefly, cetyl trimethylammonium bromide (CTAB) (0.5 g) was dissolved in water (240 mL) containing 1.75 mL of NaOH 2M. The solution was then heated up to 80°C and stirred vigorously. Meanwhile, TEOS (2.5 mL) was dissolved in absolute ethanol (3 mL), adding 50 µL of APTES and 0.1 mg of Cyanine 5-NHS ester dye (NHS-Cy5). This second solution was then added to the former CTAB flask and the final mixture was stirred overnight at 80°C. The particles were then recovered by centrifugation and washed several times with water. They were subsequently filled with TMZ by impregnation, and eventually coated with PNA, as described in the Supporting Information.

Cell cultures and assays: Rattus norvegicus brain glioma (C6 glioma) cells and human glioblastoma multiforme T98G cell line were used, according to the procedures reported in the Supporting Information Section. The procedures for nanoparticle incubation for cell uptake recording and organelle staining, fluorescence confocal microscopy experiments, cell viability test, quantitative analyses of miRNAs, analysis of apoptosis, cellular uptake by FACS analysis are reported in Supplementary Information.

Supporting Information

Supporting Information is available from the Wiley Online Library or from the author.

Acknowledgements

L. De Cola, E.A. Prasetyanto, and D.Septiadi acknowledge financial support from the European Research Council for ERC Advanced Grant (Grant Agreement no. 2009-247365). A.Bertucci and R.Corradini thank the French Embassy in Italy and the French government for providing the MAEE grant for scientific cooperation between Italy and France (number 778588G). R.Gambari and R.Corradini are grateful to the Italian Association for Cancer Research (AIRC, contract number IG13575).

Received: ((will be filled in by the editorial staff))
Revised: ((will be filled in by the editorial staff))
Published online: ((will be filled in by the editorial staff))

[1] M. M. Ottesman, *Annu. Rev. Med*. **2002**, *53*, 615.

[2] L. S. Jabr-Milane, L. E. Van Vlerken, S. Yadav, M. M. Amiji, *Cancer Treat. Rev.* **2008,** *34*, 592.

[3] M. Saraswathy, S. Gong, *Mater. Today* **2014**, *17*, 298.

[4] D. Lane *Nat. Biotechnol.* **2006**, *24*, 163.

[5] I. V. Lebedeva IV, I. Washington, D. Sarkar, J. A. Clark, R. L. Fine, P. Dent, D. T. Curiel, N. J. Turro, P. B. Fisher, *Proc. Natl. Acad. Sci. USA* **2007**, *104*, 3484.

[6] W. Zhang, Z. Guo, D. Buang, Z. Liu, X. Guo, H. Zhong, *Biomaterials* **2011**, *32*, 8555.

[7] F. Greco, M. J. Vicent, *Adv. Drug Deliver. Rev.* **2009**, *61*, 1203.

[8] M. E. Davis, J. E. Zuckerman, C. H. Choi, D. Seligson, A. Tolcher, C. A. Alabi, Y. Yen, J. D. Heidel, A. Ribas, *Nature* **2010**, 464, 1067.

[9] C. D. Porada, G. Almeida-Porada, *Adv. Drug Deliver. Rev*. **2010**, *62*, 1156.

[10] C. Zhu, S. Jung, S. Luo, F. Meng, X. Zhu, T. G. Park, Z. Zhong, *Biomaterials* **2010**, *31*, 2408.

[11] N. Cao, D. Cheng, S. Zou, H. Ai, J. Gao, X. Shuai, *Biomaterials* **2011**, *32*, 2222.

[12] M. E. Godsey, S. Suryaprakash, K. W. Leong, *RSC Advances* **2013**, *3*, 24794.

[13] N. S. Gandhi, R.K. Tekade, M. B. Chougule, *J. Control. Rel*. **2014**, *194*, 238-256.

[14] A. M. Chen, M. Zhang, D. Wei, D. Stueber, O. Taratula, T. Minko, H. He, *Small* **2009**, *5*, 2673.

[15] I.I. Slowing, J. L. Vivero-Escoto, C. W. Wu, V. S. Y. Lin, *Adv. Drug Deliver. Rev.* **2008**, *60*, 1278.

[16] Q. Zhang, X. Wang, P. Z. Li, K. T. Nguy, X. Y. Wang, Z. Luo, H. Zhang, N. S. Tan, Y.Zhao, *Adv. Funct. Mater.* **2013**, *24*, 2450.

[17] Z. Li, J. C. Barnes, A. Bosoy, J. F. Stoddart, J. I. Zink, *Chem. Soc. Rev.* **2012**, *41*, 2590.

[18] C. Argyo, V. Weiss, C. Bräuchle, T. Bein, *Chem. Mater*. **2014**, *26*, 435.

[19] M. Vallet-Regí, F. Balas, D. Arcos, *Angew. Chem. Int. Ed*. **2007**, *46*, 7548.

[20] Y. Chen, H Chen, H., J. Shi, *Adv. Mater*. **2013**, *25*, 3144.

[21] Y. Chen, H. Chen, J. Shi, *Mol. Pharm.* **2014**, *11*, 2495.

[22] P. Zhang, F. Cheng, R. Zhou, J. Cao, J .Li, C. Burda, Q. Min, J. J. Zhu, *Angew. Chem. Int. Ed*. **2014**, *53*, 2371.

[23] H. Men, W. X. Mai, H. Zhang, M. Xue, T. Xia, S. Lin. X. Wang, Y. Zhao, Z. Ji, J. I. Zink, A. E. Nel, *ACS Nano **2013***, *7*, 994.

[24] X. Ma, Y. Zhao, K. W. Ng, Y. Zhao, *Chem-Eur J*. **2013**, *19*, 15593.

[25] D. P. Bartel, *Cell* **2004***, 116*, 281.

[26] L. He, G. J. Hannon, *Nat. Rev. Genet.* **2004***, 5*, 522.

[27] G. A. Calin, C. M. Croce, *Nat. Rev. Cancer* **2006**, *6*, 857.

[28] R. Piva, D. A. Spandidos, R. Gambari, *Int. J. Oncol.* **2013***, 43*, 985.

[29] P. Pineau P, S. Volinia, K. McJunkin, A. Marchio, C. Battiston, B. Terris, V. Mazzaferro, S. W. Lowe, C. M. Croce, A. Dejean, *Proc. Natl. Acad. Sci. USA* **2010**, 107, 264.

[30] J. Radojicic, A. Zavarinos, T. Vrekoussis, M. Kafousi, D. A. Spandidos, E. N. Stathopoulos, *Cell Cycle* **2011**, *10*, 507.

[31] H. He, K. Jazdzewski, W. Li, S. Liyanarachchi, R. Nagy, S. Volinia, G. A. Calin, G. C. Liu, K. Franssila, S. Suster, R. T. Kloos, C. M. Croce, A. de la Chapelle, *Proc. Natl. Acad. Sci. USA* **2005**, *102*, 19075.

[32] J. Zhang, L. Han, Y. Ge, X. Zhou, A. Zhang, C. Zhang, Y. Zhong, Y. You, P. Pu, C. Kang, *Int. J. Oncol.* **2010**, *36*, 913.

[33] E. Brognara, E. Fabbri, E. Bazzoli, G. Montagner, C. Ghimenton, A. Eccher, C. Cantù, A. Manicardi, N. Bianchi, A. Finotti, G. Breveglieri, M. Borgatti, R. Corradini, V. Bezzeri, G. Cabrini, R. Gambari, *J. Neuro-Oncol.* **2014**, *118*, 19.

[34] C. Z. Zhang, J. X. Zhang, A. L. Zhang, Z. D. Shi, L. Han, Z. F. Jia, W. D. Yang, G. X. Wang, T. Jiang, Y. P. You, P. Y. Pu, J. Q. Cheng, C. S. Kang, *Mol. Cancer* **2010**, *9*, 229.

[35] A. Borriello, V. Cucciola, A. Oliva, V. Zappia, F. Della Ragione *Cell Cycle* **2007**, *6*, 1053.

[36] C. Zhang, C. Kang, Y. You, P. Pu, W. Yang, P. Zhao, G. wang, A. Zhang, Z. Jia, L. Han, H. Jiang, *Int. J. Oncol.* **2009**, *34*, 1653.

[37] J. K. Gillies, I. A. Lorimer, *Cell Cycle* **2007***, 6*, 2005.

[38] T. E. Miller, K. Ghoshal, B. Ramaswamy, S. Roy, J. Datta, C. L. Shapiro, S. Jacob, S. Majudmer, *J. Biol. Chem.* **2008**, *283*, 29897.

[39] L. Chen, J. Zhang, L. Han, A. Zhang, C. Zhang, Y. Zheng, T. Jiang, P. Pu, C. Jiang, C. Jang, *Oncol. Rep.* **2012***, 27*, 854.

[40] T. C. Hirst, H. M. Vesterinen, E. S. Sena, K. J. Egan, M. R. Macleod, I. R. Whittle, *Brit. J. Cancer* **2013**, *108*, 64.

[41] H. M. Strik, C. Marosi, B. Kaina, B. Neyns, *Curr. Neurol. Neurosci. Rep.* **2012***, 12*, 286.

[42] N. Falkenberg, N. Anastasov, K. Rappl, H. Braselmann, G. Auer, A. Walch, M. Huber, I. Hofig, M. Schmitt, H. Hofler, M. J. Atkinson, M. Aubele, *British J. Cancer* **2013**, *109*, 2714.

[43] C. Quintavalle, M. Garofalo, C. Zanca, G. Romano, M. Iaboni, M. del Basso De Caro, J. C. Martinez.Montero, M. Incoronato, G. Nuovo, C. M. Croce, G. Condorelli, *Oncogene* **2012***, 31*, 858.

[44] M.A. Chaudhry, *J. Cell Biochem*. **2014**, *115*, 436.

[45] P. E. Nielsen, M. Egholm, R. H. Berg, O. Buchardt, *Science* **1991**, *254*, 1497.

[46] P. E. Nielsen, *Chem. Biodivers*. **2010**, *7*, 786.

[47] J. C. Hanvey, N. J. Peffer, J. E. Bisi, S.A. Thomson, R. Cadilla, J. A. Josey, D. J. Ricca, C. F. Hassman, M. A. Bonham, K. G. Au, S, G. Carter, D. A: Bruckenstein, A. L. Boyd, S. A. Noble, L. E. Babiss, *Science* **1992**, *258*, 1481.

[48] M. M. Fabani, C. Abreu-Goodger, D. Williams, P. A. lyons, A. G. Torres, K. G. Smith, A. J. Enright, M. J. Gait, E. Vigorito, *Nucleic acids Res.* **2010**, *38*, 4466.

[49] E. Fabbri, A. Manicardi, T. Tedeschi, S. Sforza, N. Bianchi, E. Brognara, A. Finotti, G. Breveglieri, M. Borgatti, R. Corradini, R. Marchelli, R. Gambari, *ChemMedChem* **2011**, *6*, 2192.

[50] S. R. Ryoo, J. Lee, J. Yeo, H. K. Na, Y. K. Kim, H. Jang, J.H. Lee, S. W. Han, Y. Lee, V. N. Kim, D. H. Min, *ACS Nano* **2013***, 7*, 5882.

[51] E. Brognara, E. Fabbri, F. Aimi, A. Manicardi, N. Bianchi, A. Finotti, G. Breveglieri, M. Borgatti, R. Corradini, R. Marchelli, R. Gambari, *Int. J. Oncol.* **2012**, *41*, 2119.

[52] E. Fabbri, E. Brognara, M. Borgatti, I. Lampronti, A. Finotti, N. Bianchi, S. Sforza, T. Tedeschi, A. Manicardi, R. Marchelli, R. Corradini, R. Gambari, *Epigenomics* **2011**, *3*, 733.

[53] R. Corradini, S. Sforza, T. Tedeschi, F. Totsingan, A. Manicardi, R. Marchelli, *Curr. Top. Med. Chem*. **2011**, *11*, 1535.

[54] B. G. Trewyn, I. I. Slowing, S. Giri, H. T. Chen, V. S. Y. Lin, *Accounts Chem. Res.* **2007**, *40*, 846.

[55] B. G. Trewyn, V. S. Y. Lin, K. Wang, *Nat. Nanotechnol.* **2007**, *2*, 295.

[56] C. H. Lee, S. H. Cheng, Y. J. Wang, Y. C. Cheng, N. T. Chen, J. Souris, C. T. Chen, C. Y. Mou, C. S. Yang, L. W. Lo, *Adv. Funct. Mater.* **2009**, *19*, 215.

[57] F. Lu, S. H. Wu, Y. Hung, C. Y. Mou, *Small* **2009**, *5*, 1408.

[58] H. Meng, M . Liong, M . Xia, Z. Li, Z. Ji, J. I. Zink, A. E. Nel, *ACS Nano* **2010**, *4*, 4539.

[59] U. Koppelhus, T. Shiraishi, V. Zachar, S. Pankratova, P. E. Nielsen *Bioconjugate Chem.* **2008**, *19*, 1526.

[60] A. Albanese, P. S. Tang, W. C. Chan, *Annu. Rev. Biomed. Eng.* **2012**, *14*, 1.

[61] E. Climent, R. Martínez-Máñez, F. Sancenón, M.D. Marcos, J. Soto, A. Maquieira, P. Amorós, *Angew. Chem.* **2010**, *122*, 7439.

[62] H. Lülf, A. Bertucci, D. Septiadi, R. Corradini, L. De Cola, *Chem-Eur. J.* **2014**, *20*, 10900.

[63] U. Koppelhus, P. E. Nielsen, *Adv. Drug Deliver. Rev.* **2003**, *55*, 267.

[64] M. Zhu, G. Nie, H. Meng, T. Xia, A. Nel, Y. Zhao, *Accounts Chem. Res*. **2012**, *46*, 622.

[65] D. Tarn, C.E. Ashley, M. Xue, E.C. Carnes, J.I. Zink, C.J. Brinker, *Accounts Chem. Res*. **2013**, *46*, 792.

[66] T. Xia, M. Kovochich, M. Liong, H. Meng, S. Kabehie, S. George, J. I. Zink, A. E. Nel, *ACS Nano* **2009**, 3, 3273.

[67] Y. Wang, X. Wang, J. Zhang, G. Sun, H. luo, C. Kang, P. Pu, T. Jiang, N. Liu, Y. You, *J. Neuro-Oncol.* **2012**, *106,* 217.

[68] J. K. Kim, K. J. Choi, M. Lee, M. H. Jo, S. Kim, *Biomaterials* **2012**, *33*, 207.

[69] T. Kato, A. Natsume, H. toda, H. Iwamizu, T. Sugita, R. Hachisu, R. watanabe, K. Yuki, K. Motomura, K. Bankiewicz, T. Wakabayashi, *Gene Ther.* ***2010***, *17*, 1363.

[70] H. Zhang, S. Gao, *Int. J. Pharm.* **2007**, *329*, 122.

[71] S. Ni, X. Fan, J. Wang, H. Qi, X. Li *Ann. Biomed. Eng*. **2014**, *42*, 214.

[72] G. H. Stein, *J. Cell Physiol.* **1979**, *99*, 43.

[73] A.G. Torres, M.M. Fabani, E. Vigorito, M.J. Gait, *RNA* **2011**, 933-943.

[74] X. Huang, X. Teng, D. Chen, F. Tang, J. He, *Biomaterials* **2010**, *31*, 438.

[75] F. Tang, L. Li, D. Chen, *Adv. Mater.* **2014**, *24*, 1504.

[76] Z. Lwin, D. MacFadden, A. Al-Zaharani, E. Atenafu, B. A. Miller, A. Sahgal, C. Menard, N. Lapierre, W. P. Mason, *J Neurooncol.* **2013**, *115*, 303.

[77] R. Stupp, M. E. Hegi, W. P. Mason, M. J. van den Bent, M. J. Taphoorn, R. C Janzer, S. K. Ludwin, A. Allgeier, B. Fisher, K. Belanger, P. Hau, A. A. Brandes, J. Gijtenbeek, C. Marosi, C. J. Vecht, K. Mokhtari, P. Wesseling, S. Villa, *et al., Lancet Oncol.* **2009**, *10*, 459.

[78] H. L. A. Janssen, H. W. Reesink, E. J. Lawitz, S. Zeuzem, M. Rodriguez-Torres, K. Patel, A. J. van der Meer, A. K. Patick, A. Chen, Y. Zhou, R. Persson, B. D. King, S. Kauppinen, A. A. Levin, M. R. Hodges, *New Engl. J. Med.* ***2013***, *386*, 1685.

[79] L. Wu, X. Li, D. R. Janagam, T. L. Lowe, *Pharm. Res.* **2014**, *31*, 531.

[80] J. Lu, M. Liong, Z. Li, J. I. Zink, F. Tamanoi, *Small* **2010**, *6*, 1794.

[81] W.A. Banks, *Peptides* **2015**, doi:10.1016/j.peptides.2015.03.010.

[82] D. Lac, U. Bhardwaj, H. Baek, A. Jang, W. Xiao, B. Le, G. Fung, E. Sanchez, K. S. Lam, *FASEB J*. **2013**, *27*, 589.

[83] A. Manicardi, A. Calabretta, M. Bencivenni, T. Tedeschi, S. Sforza, R. Corradini, R. Marchelli, *Chirality* **2010**, *22*, E161.

[84] K. K. Coti, M. E. Belowich, M. Liong, M. W. Ambrogio, Y. A. Lau, H. A. Khatib, J. I. Zink, N. M. Khashab, J. F. Stoddart, *Nanoscale* **2009**, *1*, 16.

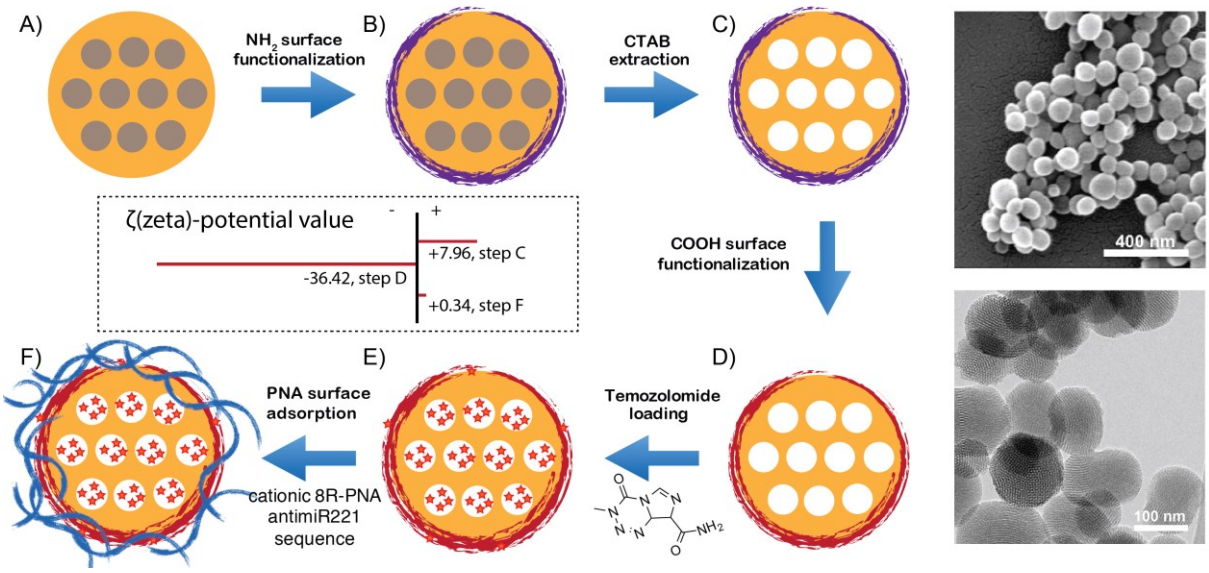

Figure 1. Functionalization and characterization of MSNPs. Left panel: schematic procedure for the functionalization of PNA-TMZ-MSNPs. After the surfactant-templated synthesis of MSNPs (A), amine groups are first introduced on the particle surface by silanization (B); CTAB is then extracted (C); the amine groups are converted into carboxylic groups by reaction with succinic anhydride (D), temozolomide is loaded in the pore system by impregnation (E); the cationic R8-PNA221 is adsorbed on the particle outer surface (F). Right panel, characterization of the material; above: SEM image of the obtained MSNPs (top); high-resolution TEM image of MSNPs after CTAB removal (C), showing the nanochannels pattern and dimensions (bottom).

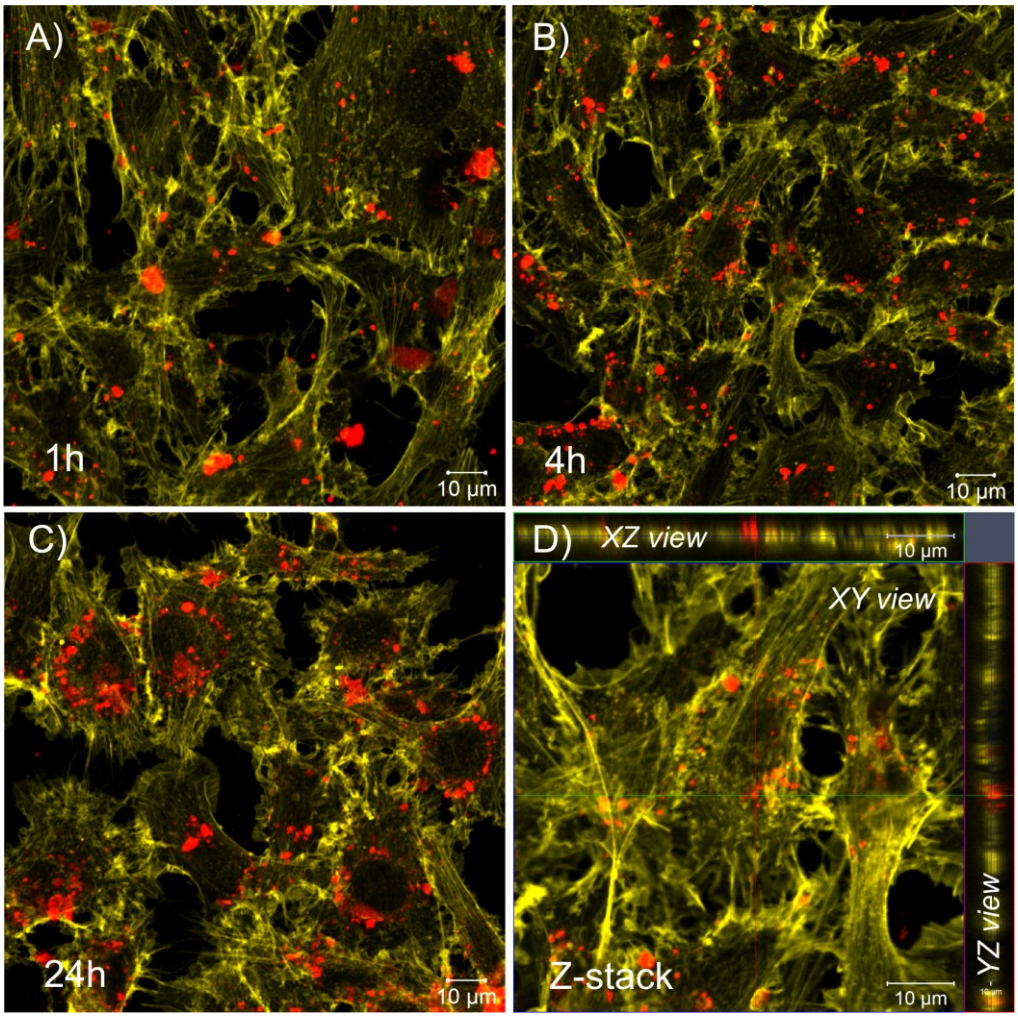

Figure 2. Confocal micrographs of C6 glioma cells incubated with 0.05 mg/mL dispersion of PNA-TMZ-MSNPs. A) 1 hour incubation; B) 4 hours incubation, C) 24 hours incubation, D) Z-stack showing 3D particle internalization after 1h incubation. The red spots refer to the emissive Cy5 dye contained in the PNA-TMZ-MSNPs, excited at 633 nm, while F-actin filaments are visualized in yellow after Alexa Fluor® 568 Phalloidin staining and excited at 543 nm.

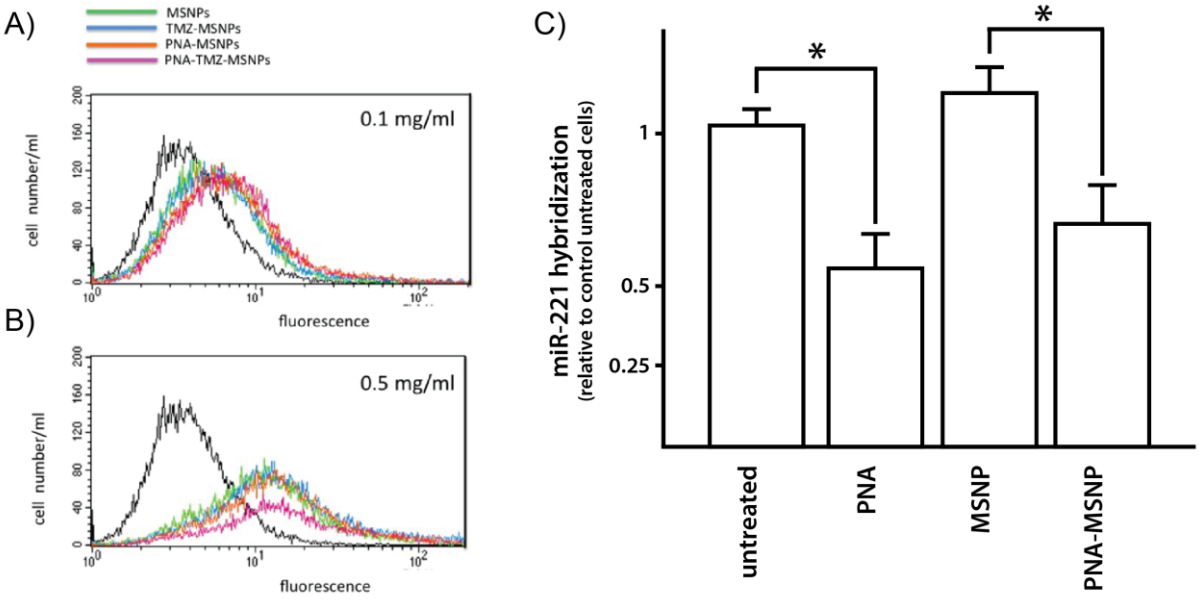

Figure 3. Uptake and anti-miR activity of PNA-MSNPs in T98G cells. Left: FACS analysis on T98G cells cultured with MSNP-based formulations. T98G cells were cultured for 24 hours in the absence of treatments (black lines), with 0.1 (A) and 0.5 (B) mg/ml: MSNPs (green lines), TMZ-MSNPs (blue lines), PNA-MSNPs (orange lines) or TMZ-PNA-MSNPs (purple lines). Right (C) miR-221 levels in T98G cells treated with PNA-MSNPs. T98G cells were cultured for 48 hours in the presence of 0.25 mg/ml MSNP, 0.25 mg/ml PNA-MSNP or 2 μM R8-PNA221, the RNA was extracted and qRT-PCR miR221 detection was performed and compared to control untreated cells. Vertical bars represent standard deviations. Asterisks indicate significant differences ($p<0.05$).

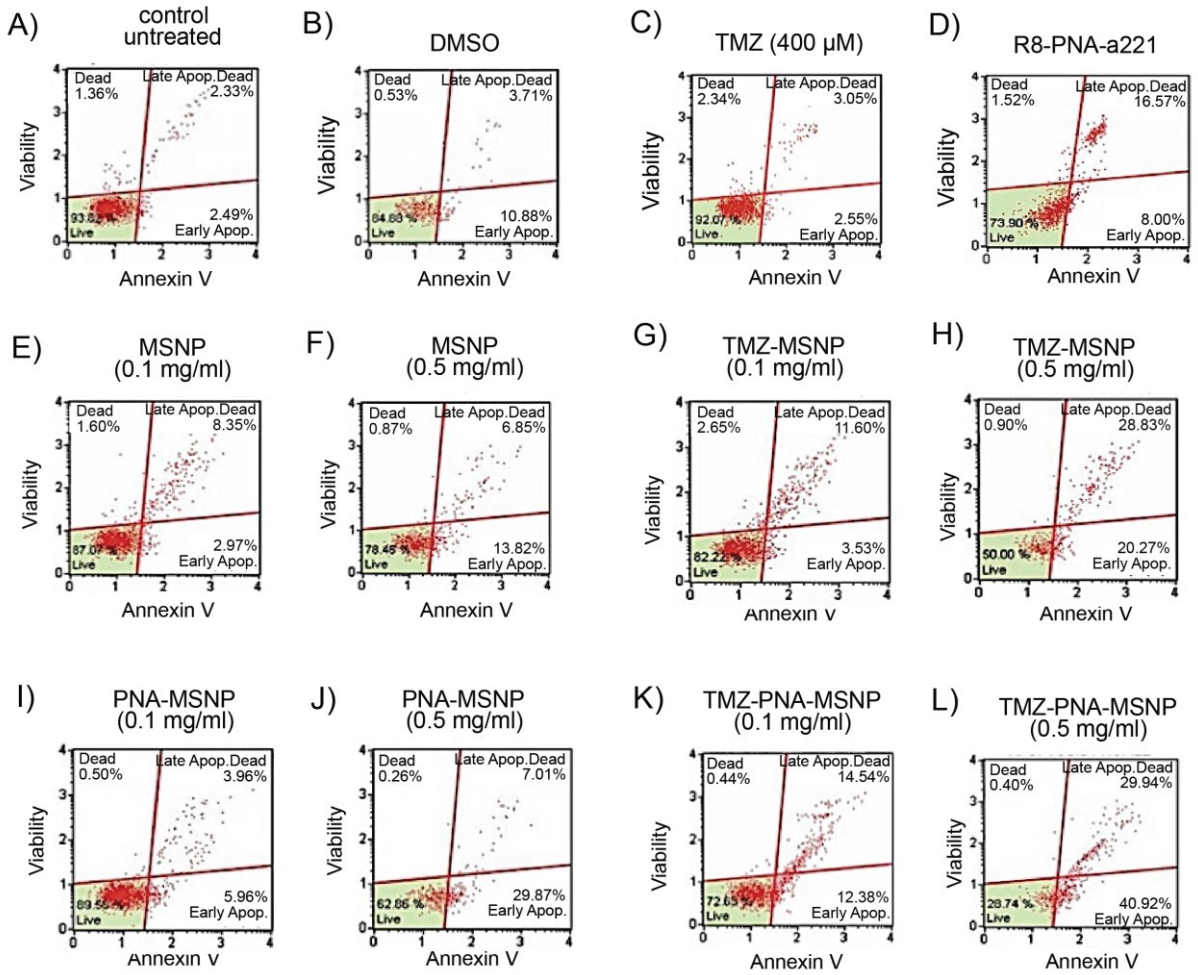

Figure 4. Induction of apoptosis of glioma T98G cells by MSNPs-based treatments. T98G cells were cultured for 48 hours in the absence of treatments (A), with 12.5 µl DMSO (B), 400 µM TMZ (C), 2 µM R8-PNA221 (D), 0.1 (E) and 0.5 (F) mg/ml MSNPs, 0.1 (G) and 0.5 (H) mg/ml TMZ-MSNPs, 0.1 (I) and 0.5 (J) mg/ml PNA-MSNPs, or 0.1 (K) and 0.5 (L) mg/ml PNA-TMZ-MSNPs. After these treatments, cells were isolated and apoptosis was determined using Annexin V exclusion test, as described in the Experimental section. Representative results obtained using the "Muse"TM (Millipore Corporation, Billerica, MA, USA) method are presented. This procedure utilizes Annexin V to detect PS (Phosphatidyl Serine) on the external membrane of apoptotic cells.

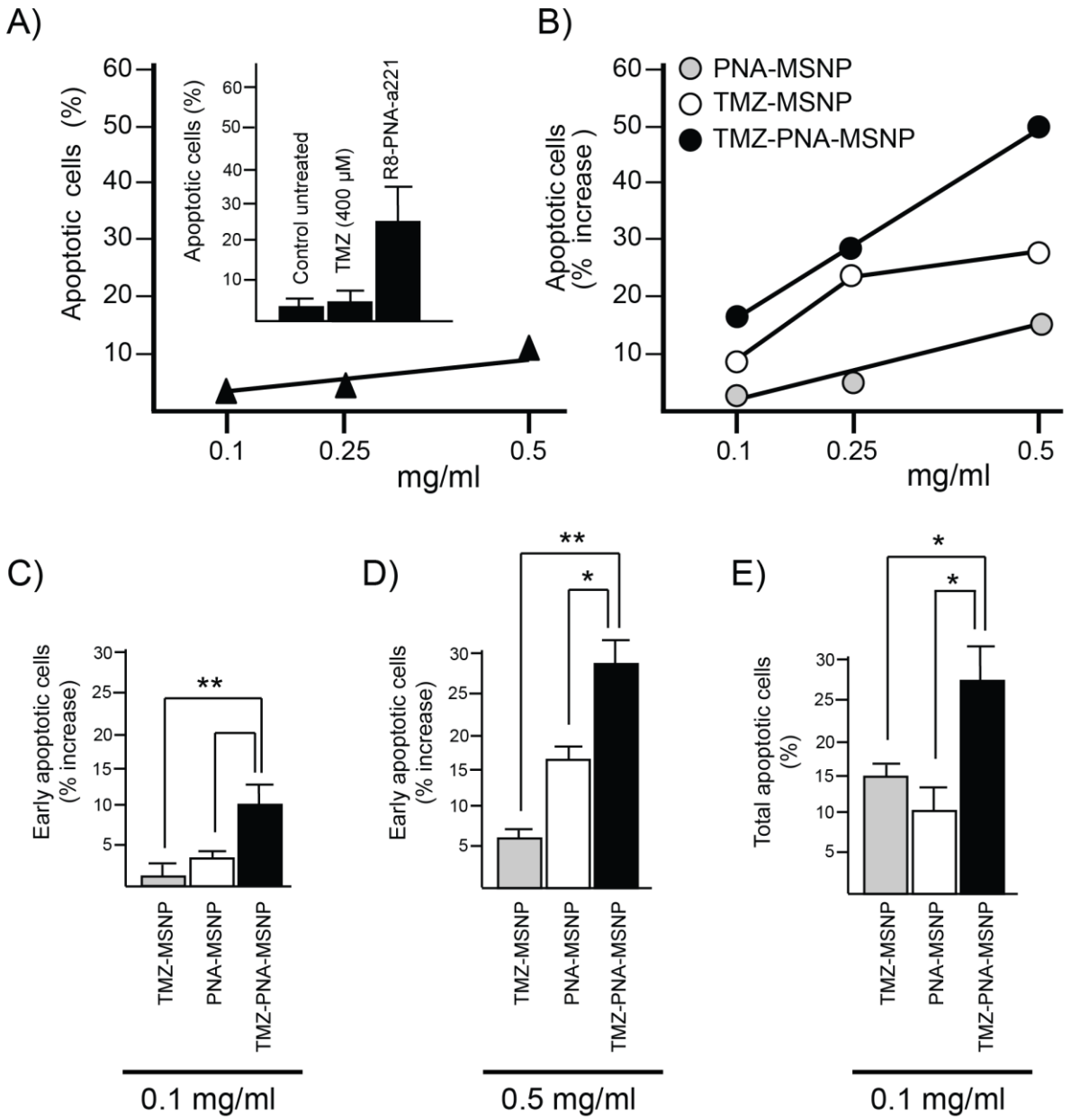

Figure 5. Summary of the results obtained on the effects of MSNP-based treatments on T98G cell apoptosis. T98G cells were treated for 48 hours as indicated in the legend to Figure 4. A. Effects on apoptosis of increasing amounts of unloaded MSNP. In the insert the proportions of apoptotic cells in untreated T98G cell populations, as well as in TMZ- or R8PNA-a221 treated cells are reported. B. Induction of apoptosis of treatments of T98G cells with increasing amounts of TMZ-MSNPs, PNA-MSNPs, or PNA-TMZ-MSNPs, as indicated. The results represent the average of three experiments. Statistics relative to induction of early

apoptotic cells and total apoptotic cells shown in panels C-E. Vertical bars represent standard deviations. Asterisks indicate significant differences (*, $p<0.05$; **, $p<0.01$)

Multifunctional mesoporous silica nanoparticles (MSNP) were used for glioblastoma treatment, harnessing drug delivery and miRNA targeting. MSNPs were synthesized and loaded with the anti-cancer drug temozolomide (TMZ), while the particle surface decorated with a polyarginine-peptide nucleic acid conjugate (R8-PNA) targeting miR221. The simultaneous effect of TMZ and R8-PNA showed a dramatic impact (70.9% of apoptotic cells) on the human T98G tumor cell line.

Keyword: drug resistance, microRNA, nanomaterials, nanomedicine, PNA

Alessandro Bertucci, Eko Adi Prasetyanto, Dedy Septiadi, Alex Manicardi, Eleonora Brognara, Roberto Gambari*, Roberto Corradini*, Luisa De Cola*

Combined delivery of temozolomide and anti-miR221 PNA using mesoporous silica nanoparticles induces apoptosis in resistant glioma cells

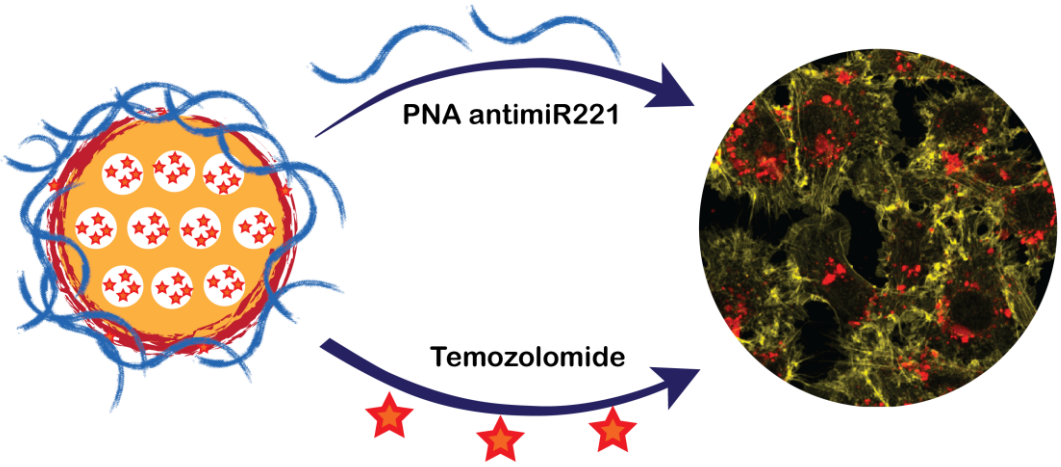

Supporting Information

Combined delivery of temozolomide and anti-miR221 PNA using mesoporous silica nanoparticles induces apoptosis in resistant glioma cells

Alessandro Bertucci, Eko Adi Prasetyanto, Dedy Septiadi, Alex Manicardi, Eleonora Brognara, Roberto Gambari, Roberto Corradini*, Luisa De Cola**

1. Chemicals

All chemicals were commercially available and used without further purification. Succinic anhydride, temozolomide, dimethyl sulfoxide (DMSO), hydrochloric acid, (3-aminopropyl)-triethoxysilane (APTES), phosphate buffered saline tablets were purchased by Sigma Aldrich (France). Cetyl trimethylammonium bromide (CTAB), tetraethyl orthosilicate (TEOS), 3-Aminopropyl-dimethyl-ethoxy silane (APDMS) were purchased by Acros Organics. All Boc-protected PNA monomers were purchased by ASM (Germany). HBTU was supplied by Matrix Innovation (Canada). MBHA resin was purchased by Merck (Italy). Cyanine 5 NHS-ester was supplied by Lumiprobe. Ultra-pure water (Milli-Q Element, Millipore) was used for all the experiments.

2. Instrumentations

SEM measurements were done using a FEI Quanta FEG 250 instrument. Zeta-potential analyses were performed on a Delsa Nano C Particle Analyzer (Beckman Coulter, Brea, CA, USA); all the measurements were conducted in phosphate buffered saline (PBS, pH = 7). All the instrumentation used for the PNA synthesis are reported in the experimental section or

elsewhere[1]. All fluorescence images of cells were obtained by using Zeiss LSM 710 confocal microscope system with 63X magnification, numerical aperture 1.3 of Zeiss LCI Plan-NEOFLUAR water immersion objective lens (Zeiss GmbH, Germany).

UV/Vis spectroscopy: Shimadzu UV3600 (Shimadzu Europe, Duisburg, Germany).

Fluorescence spectroscopy: Steady-state emission spectra were recorded on a HORIBA Jobin-Yvon IBH FL-322 Fluorolog 3 spectrometer equipped with a 450 W xenon arc lamp as the excitation source, double-grating excitation and emission monochromators (2.1 nm mm−1 of dispersion; 1200 grooves mm−1), and a TBX-04 single-photon-counting device as the detector.

Small-angle/Wide-angle X-ray Scattering (SAXS/WAXS): SAXS/WAXS measurements of samples were performed with SAXSess Small-angle X-Ray Scattering instrument (Anton Paar GmbH, Austria). The Kratky type camera is attached to a laboratory X-Ray generator (PW3830, PANalytical), and was operated with a fine focus glass sealed X-Ray tube at 40 kV and 50 mA (Cu Kα, α = 0.1542 nm). Detection was performed with the 2D imaging plate and analyzed by an imaging plate reader Cyclone® (Perkin Elmer). Powder samples were held in tape, and the tape background was subtracted before desmearing the data using the Lake method to account for the slit shaped beam. The two-dimensional intensity data were converted to one-dimensional data with SASXQuant software (Anton Paar GmbH, Austria).

Cell counter and cytotoxicity equipment: CASY Model TT – Cell Counter and Analyzer (Roche Innovatis AG)

3.Synthesis of cationic anti-miR-221 PNA (8R-PNA221)

The cationic anti-miR-221 PNA H-RRRRRRRR-GCAGACAATGTAGCT-Gly-NH_2 (where R is an arginine residue) was synthesized with standard manual Boc-based chemistry using commercially available monomers, with HBTU/DIPEA coupling as described elsewhere.[2] The synthesis was carried out in a 10 μmol scale using MBHA resin. The R8 cationic arginine

tail was introduced using the same coupling procedures. PNA purification was performed by RP-HPLC with UV detection at 260 nm using a semi-prep column C18 (10 μm, 7.8x300 mm, Xterra Waters), eluting with water containing 0.1% TFA (eluent A) and acetonitrile containing 0.1% TFA (eluent B); elution gradient: from 100% A to 50% B in 30 min, flow: 4 mL/min. The resulting pure PNA oligomer was characterized by ESI-MS, which gave positive ions consistent with the final products: m/z found (calcd) 1084.5 (1084.5) $[M+5H]^{5+}$, 903.7 (903.9) $[M+6H]^{6+}$, 774.7 (774.9) $[M+7H]^{7+}$, 678.0 (678.2) $[M+8H]^{8+}$, 602.9 (602.9) $[M+9H]^{9+}$, 542.4 (542.7), $[M+10H]^{10+}$.

4. Synthesis of red-fluorescent MSNPs (Cy5-MSNPs)

Cetyl trimethylammonium bromide (CTAB) (0.5 g) was dissolved in water (240 mL) containing 1.75 mL of NaOH 2M. The solution was then heated up to 80°C and stirred vigorously. Meanwhile, TEOS (2.5 mL) was dissolved in absolute ethanol (3 mL), adding 50 μL of APTES and 0.1 mg of Cyanine 5-NHS ester dye (NHS-Cy5). This second solution was then added to the former CTAB flask and the final mixture was stirred overnight at 80°C. The particles were then recovered by centrifugation and washed several times with water.

5. Amine-functionalization of MSNPs

3-Aminopropyl-dimethyl-ethoxy silane (APDMS) (150 μL) was added to a dispersion of 400 mg of MSNPs in ethanol, together with a catalytic amount of TEA. The mixture was then stirred overnight at room temperature. The particles were recovered by centrifugation and washed several times with ethanol.

6. Removal of CTAB from the pores

To remove CTAB from MSNP pores, the particles were shaken overnight with ethanol containing few drops of HCl 37%.

Afterwards, they were recovered by centrifugation and washed several times with ethanol and water.

7. Carboxylate-functionalization of MSNPs (COOH-MSNPs)

MSNPs (80 mg) were dispersed in DMSO (10 mL), then succinic anhydride (100 mg) was added, and the mixture was stirred overnight at room temperature. The material was then recovered by centrifugation and washed three times with DMSO and twice with water.

8. Temozolomide loading (TMZ-MSNPs)

COOH-MSNPs (20 mg) were dispersed in 5 mL of methanol and 15 mg of temozolomide (TMZ) were added. The mixture was thoroughly sonicated to get a homogenous dispersion and then stirred overnight at room temperature. Methanol was then directly evaporated under vacuum, and the particles were washed at first with methanol to remove the TMZ physically adsorbed on the MSNP surface, then several water washings were applied to further purify the material. To evaluate temozolomide loading capacity, the washing solutions were collected and the residual drug content was calculated by UV-Vis measurements at the wavelength λ = 328 nm. A calibration curve by standard solutions of temozolomide in methanol was built up to allow for quantification, whose equation is $y = 56.343x$. The linear model has been validated by Mandel test (figure S5). A quantity of 3.4 mg temozolomide per 20 mg MSNPs has thus been calculated, which indicates a loading value of 17% (*wt/wt*).

9. PNA-functionalization of MSNPs (PNA-MSNPs)

TMZ-MSNPs or COOH-MSNPs (10 mg) were dispersed in 1 mL of a 90 μM aqueous solution of R8-PNA221, and the mixture was stirred at room temperature for 4 hours. Afterwards, the material was recovered by centrifugation and washed with water.

10. Glioma cell culture

Rattus norvegicus brain glioma (C6 glioma) cells were cultured inside media containing 88% Dulbecco's Modified Eagle Medium (DMEM), 10% Fetal Bovine Serum (FBS), 1% Penicillin-Streptomycin and 1% L-Glutamine 200mM (all materials for cell culture were purchased from Gibco), under 37°C and 5% of CO_2 condition for 48 hours until reaching 80 to 90% cell confluency. Successively, the cells were washed twice with Phosphate Buffer Solution (PBS), trypsinized and approximately 50,000 cells were reseeded on the rectangular glass cover slip (VWR) inside six-well plate culture dish. 2 ml of fresh culture media was added gently and cells were grown overnight.

Human glioblastoma multiforme T98G cell line[3] was cultured in humidified atmosphere of 5% CO_2/air in RPMI 1640 medium (Life Technologies, Monza, Italy) supplemented with 10% fetal bovine serum (FBS, Celbio, Milan, Italy), 100 units/ml penicillin and 100 mg/ml streptomycin.

11. Nanoparticle incubation for cell uptake recording and organelle staining

The initial growth serum was removed and 1 mL of 0.05 mg/ml dispersion of nanoparticle in fresh culture medium was gently added onto cells. Incubation period was done for 1, 4, and 24 hours. After incubation at 37°C and 5% of CO_2, the media was removed and the cell layer on glass cover slips was gently washed (three times) with PBS and fixed with 4% paraformaldehyde (PFA) solution for 10 minutes. Next, cell layer was washed twice with PBS and kept in 0.1% Triton X-100 in PBS for 5 minutes and afterwards in 1% bovine serum

albumin, BSA (Sigma Aldrich), in PBS for 20 minutes. The cell layer on glass cover slip was stained with Phalloidin Alexa Fluor® 568 (Invitrogen), for F-actin/membrane staining, for 20 minutes, in the dark at room temperature, and washed twice with PBS and one time with water. The cover slips were mounted onto glass slides for microscopy measurements.

12. Fluorescence confocal microscopy experiments

All depicted fluorescence microscopy images were acquired by using Zeiss LSM 710 confocal microscope system with 63 times magnification, numerical aperture 1.3 of Zeiss LCI Plan-NEOFLUAR water immersion objective lens (Zeiss GmbH). The CY5 modified particles inside the cells were excited by a continuous wave (cw) laser at 633 nm while for the cells priorly co-stained with Alexa Fluor® 568 Phalloidin dye (excitation/emission wavelength: 578 nm/600 nm) were excited independently at 543 nm, respectively. The emission of the particles and Alexa Fluor® 568 Phalloidin were collected using their corresponding emission filter. All image processing was proceeded by ZEN software (Zeiss GmbH). False color images were adjusted to better distinguish the particles and cellular organelles (F-actin).

13. Cell viability test

Cell viability test on C6 glioma cells was conducted based on non-invasive Electrical Current Exclusion (ECE) principal using an automatic CASY cell counting (Roche Innovatis AG). Approximately 50,000 cells were grown in 2 ml of fresh media inside 6 well plates at 37ºC, 5% CO_2 environment overnight. The serum was removed and replaced independently with 1 ml of the nanoparticle dispersion respectively, namely TMZ-MSNPs, PNA-MSNPs, and PNA-TMZ-MSNPs (concentration 0.17 mg/mL). Subsequently, after 24 and 48 hours of incubation, the nanoparticle solutions were removed to Eppendorf tubes and 0.5 ml of trypsin-EDTA 0.25% (Invitrogen) were added. Cells were detached from the surface by rinsing for 5

minutes in the same condition explained before. Next, 0.5 ml of pure medium was added to neutralize trypsin. Cell suspensions were collected into the same Eppendorf tube and gently mixed. 100 µl of the cell suspension was dissolved in 10 ml of CASY-ton solution (Roche Innovatis AG) and measurement was performed. The results are reported in Figure S6 (1 day) and S7 (2 days).

14. RNA extraction

Cultured cells were trypsinized and collected by centrifugation at 1,500 rpm for 10 min at 4 °C, washed with PBS, lysed with Tri-ReagentTM (Sigma Aldrich, St.Louis, Missouri, USA), according to manufacturer's instructions. The isolated RNA was washed once with cold 75% ethanol, dried and dissolved in nuclease free pure water before use.

15. Quantitative analyses of miRNAs

Reverse transcriptase (RT) reactions were performed using the TaqMan® MicroRNA Reverse Transcription Kit (Applied Biosystems, Foster City, CA, USA); real-time PCR was performed according to the manufacturer's protocols. Twenty ng per sample were used for the assays. All RT reactions, including no-template controls and RT-minus controls, were performed in duplicate using the CFX96 Touch™ Real-Time PCR Detection System (Bio-Rad Laboratories, Milan, Italy). The relative expression was calculated using the comparative cycle threshold method and as reference U6 snRNA was used to normalize all RNA samples, since it remains constant in the assayed samples by miR-profiling and quantitative RT-PCR analysis, as previously reported.[4]

16. Analysis of apoptosis

Annexin V and Dead Cell assay on T98G cell line, untreated and treated for 48 h with different concentrations of temozolomide, R8-PNA-a221 and MSNPs, were performed with

"Muse"TM (Millipore Corporation, Billerica, MA, USA) method, according to the instructions supplied by the manufacturer. This procedure utilizes Annexin V to detect PS (Phosphatidyl Serine) on the external membrane of apoptotic cells. A dead cell marker is also used as an indicator of cell membrane structural integrity. It is excluded from live, healthy cells, as well as early apoptotic cells. Four populations of cells can be distinguished in this assay. Cells were washed with sterile PBS 1X, trypsinized, suspended and diluted (1:2) with the one step addition of the Muse™ Annexin V & Dead Cell reagent. After incubation of 20 min at room temperature in the dark, samples were analyzed. Data from prepared samples are acquired and recorded utilizing the Annexin V and Dead Cell Software Module (Millipore).

17. Cellular uptake by FACS analysis

T98G cells were culture in presence of MSNPs at 0.1 and 0.5 mg/ml concentrations for 24 hours. After incubation, for the determination of the cellular fluorescence intensity a FACScan (Becton Dickinson) was used. Cells were harvested and washed; then 20000 cells were analyzed using the Fl2 channel to detect red fluorescence and the Cell Quest Pro software to analyze the data. The results were expressed as median fold, the ratio between the median of fluorescence intensity values obtained by cells in the presence and in the absence of treatment, respectively; also the MPF% (Median Peak Fluorescence %), expressing the increase % of the fluorescence value caused by the inducer molecule, could be used. A graphic presentation of data was finally obtained both by histograms, showing the number of cells versus the fluorescence intensity expressed (Fl2), and cytograms, showing the sideward light scatter (SSC) versus either the forward light scatter (FSC) or the fluorescence intensity (Fl2).

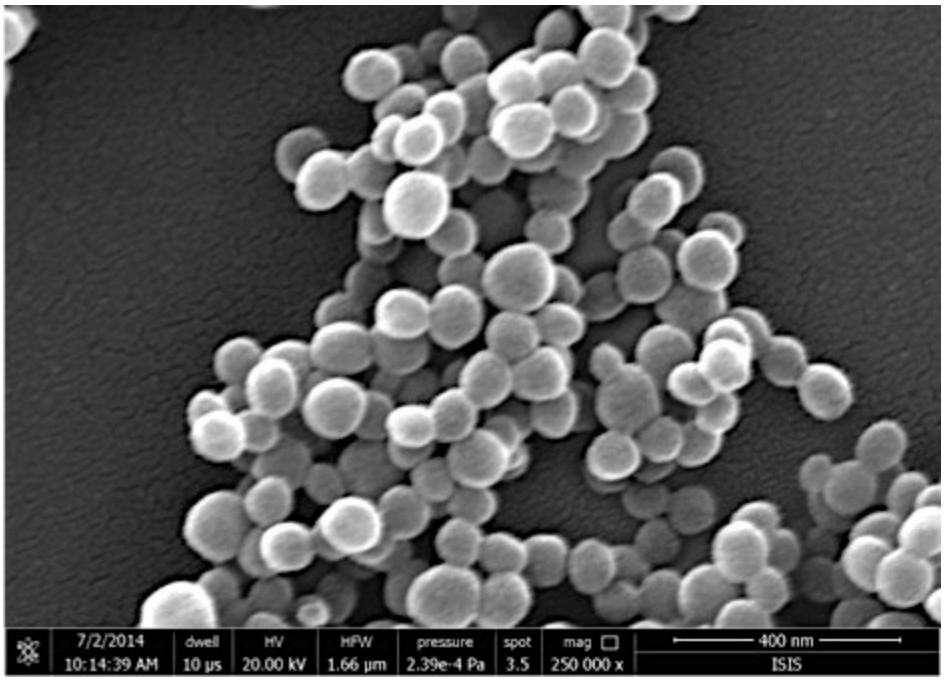

Figure S1. SEM picture of MSNPs

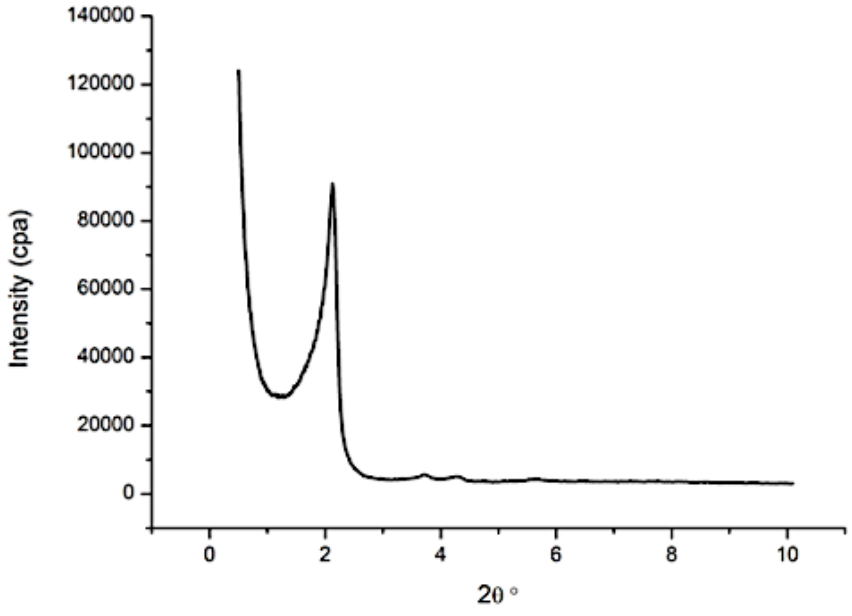

Figure S2. SAXS graph of MSNPs.

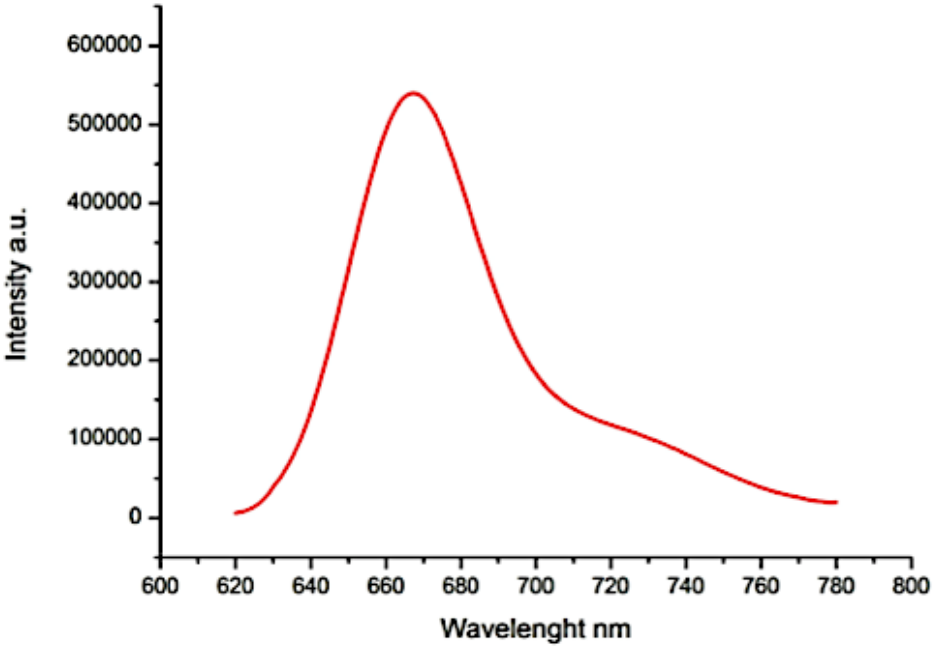

Figure S3. Emission spectrum of the particle dispersion in ethanol (λ_{exc} = 600 nm).

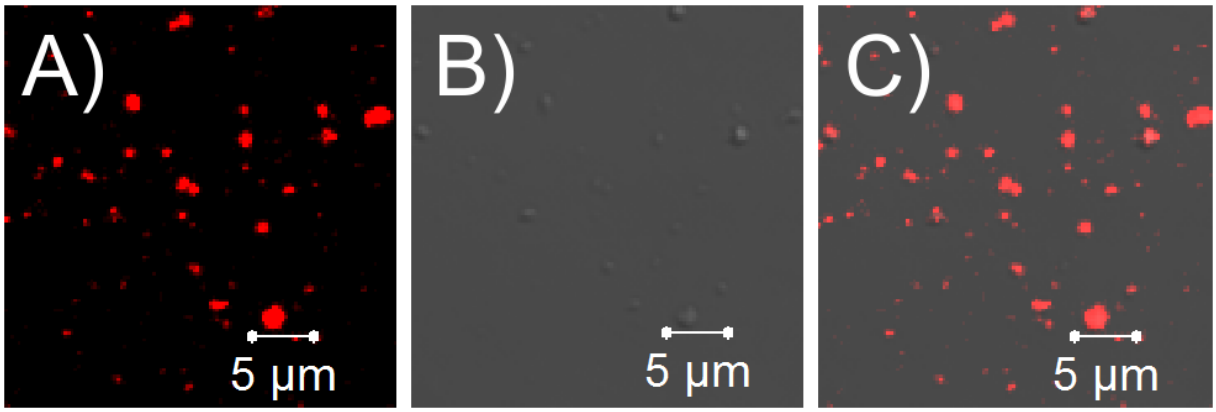

Figure S4. Confocal micrographs showing Cy5-MSNPs. A) Cy5 emission; B) brightfield image; C) Overlay. The particles are excited using λ_{exc} = 633 nm.

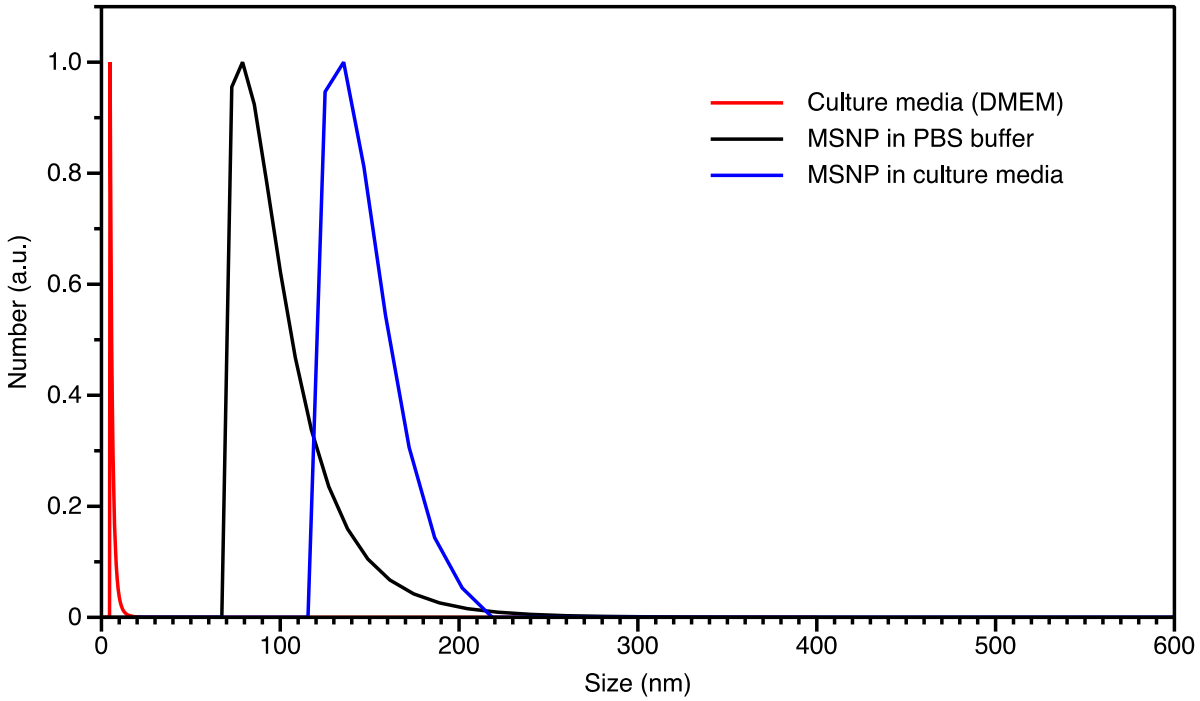

Figure S5. DLS curves showing size distribution of MSNPs in PBS buffer and culture media. The culture media environment seems to induce a slight shift of the size distribution of the particles that might be induced by interactions mediated by the presence of the serum proteins.

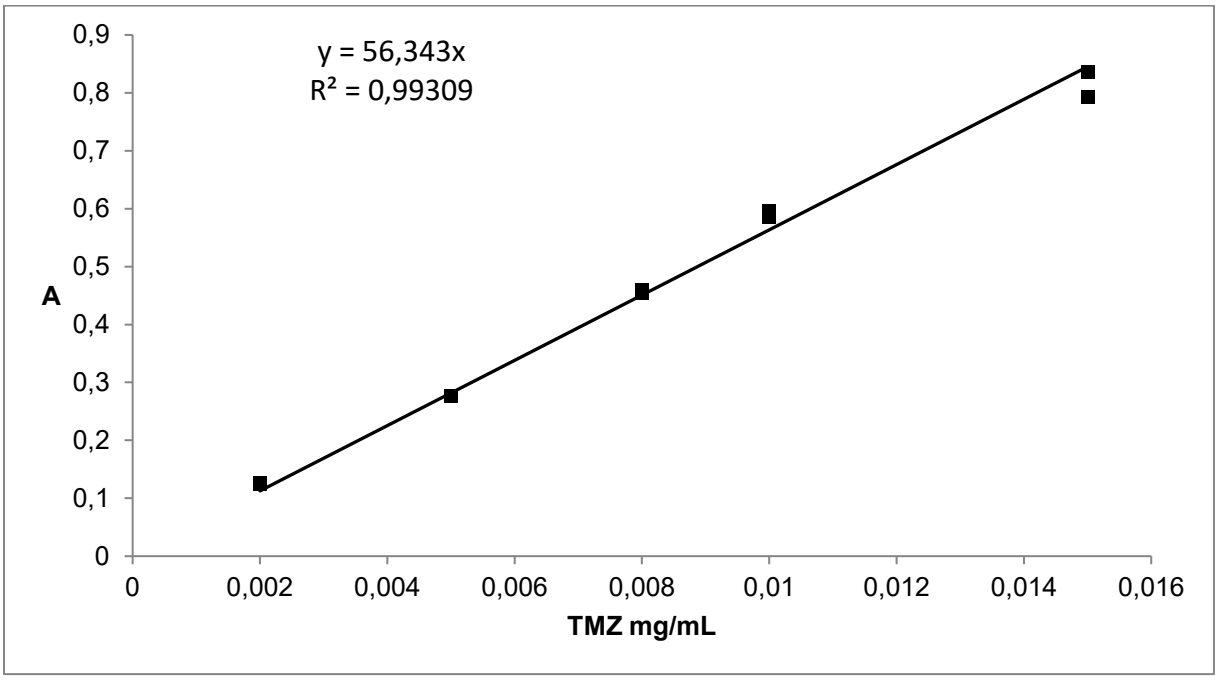

Figure S6. Calibration curve for temozolomide in methanol. Absorbance values were recorded at λ = 328 nm.

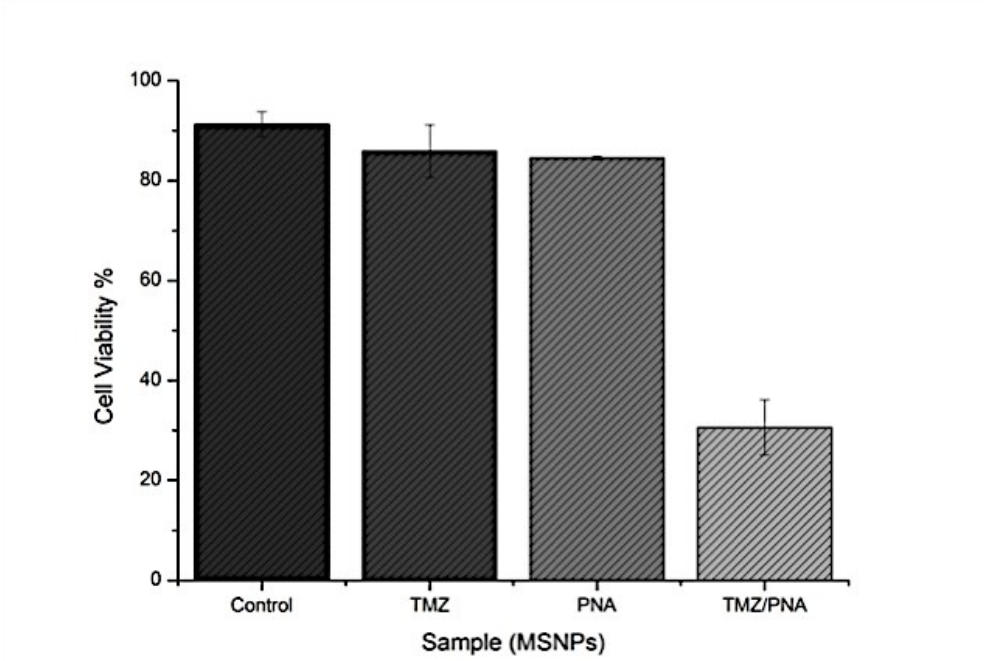

Figure S7. Cell viability values obtained after 24 hours of incubation for C6 glioma. Control (pure cell culture) 91.3% , TMZ-MSNPs 85.9%, PNA-MSNPs 84.6%, PNA-TMZ-MSNPs 30.6%. All experiments were reproduced in triplicate.

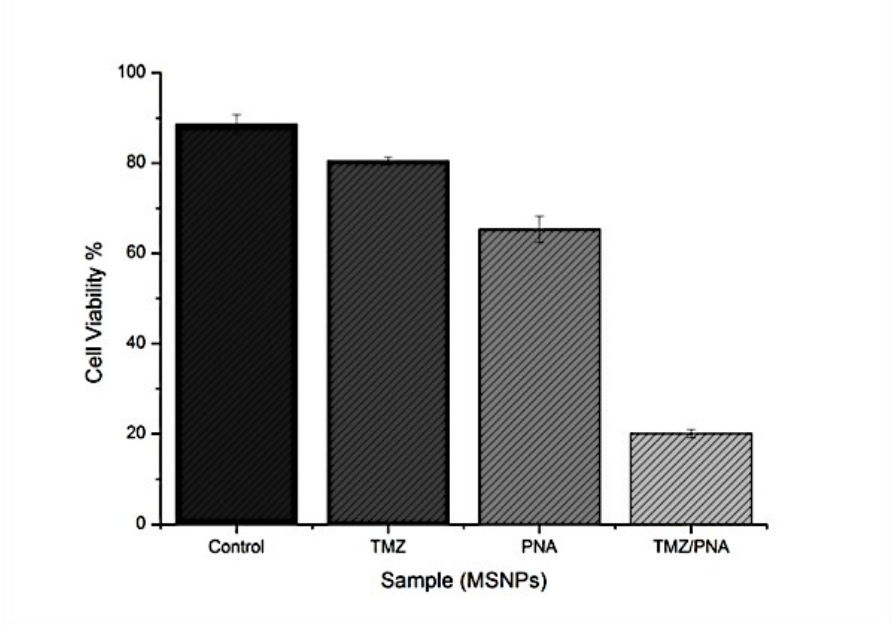

Fig. S8. Cell viability values obtained after 48 hours of incubation for C6 glioma. Control (pure cell culture) 88.6%, TMZ-MSNPs 80.5%, PNA-MSNPs 65.3%, PNA-TMZ-MSNPs 20.1%. All experiments are reproduced in triplicate.

References:

[1] A. Manicardi, E. Fabbri, T. Tedeschi, S. Sforza, N. Bianchi, E. Brognara, R. Gambari, R. Marchelli, R. Corradini, *ChemBioChem* **2012***, 13*, 1327.

[2] A. Manicardi, A. Calabretta, M. Bencivenni, T. Tedeschi, S. Sforza, R. Corradini, R. Marchelli, *Chirality* **2010***, 22*, E161.

[3] G. H. Stein, *J. Cell. Physiol.* **1979**, *99*, 43.

[4] E. Brognara, E. Fabbri, F. Aimi, A. Manicardi, N. Bianchi, A. Finotti, G. Breveglieri, M. Borgatti, R. Corradini, R. Marchelli, R. Gambari, *Int. J. Oncol.* **2012**, *41*, 2119.